

# Experimental and Numerical Study of Effective Wake of a Ship

J.W. Park<sup>1</sup>, J.J. Kim<sup>1</sup>, D.S. Kong<sup>1</sup> and J.M. Lew<sup>2</sup>

<sup>1</sup>Samsung Heavy Industries, Shipbuilding & Plant Research Institute

<sup>2</sup>Chungnam National University, Department of Naval Architecture and Ocean Engineering;  
E-mail: jmllew@cnu.ac.kr

## Abstract

LDV measurements in large cavitation tunnel around a propeller in operation are carried out to provide valuable information for more accurate wake-adapted propeller design and to study hull-propeller interactions. Effective velocities are computed by both the simplified vortex ring method and by RANS solver with the body force representing the propeller load. The former method uses the nominal velocities measured at the propeller plane as an input data of the numerical method and shows a better agreement with experimental data. The latter shows the qualitative agreement and may be used as an alternative design tools in the preliminary design stage.

**Keywords:** LDV, large cavitation tunnel, hull-propeller interactions, vortex ring method, RANS solver with body force

## 1 Introduction

To improve the propulsive performance of a ship, it is essential to understand the interaction effects among the hull, propeller and the rudder. Accurate prediction of effective velocities around propeller is also important for an improvement of the design of stern hull form and/or wake-adapted propellers. Stern et al (1994) computed hull and propeller interactions by solving Navier-Stokes equations with a propeller as body-force generator. As an alternative approach, Huang and Groves (1980), Breslin et al (1980) and Lee et al (1990) computed the effective wake of a simple body which is defined as a form of volume integrals of induced velocities due to the vortices contained in the stern shear flow and used the predetermined vortex tube contraction model.

Total velocity data around the propeller is an essential information in predicting the effective wake and the experimental data with the propeller in action is rare, especially for the practical hull form. In the present study, LDV measurements in large cavitation tunnel around a propeller in operation are carried out for practical container hull form. Effective velocities are also computed by the simplified vortex ring method and by RANS solver with body force distribution method. Numerical results of different computational approaches are compared with the experiments. It is found that both approaches can be used in initial propeller/hull design stage.

**Table 1:** Principal characteristics of model ship and model propeller

Model		Model Propeller	
$L_{pp}$	8,278 mm	Diameter	250 mm
$B$	1,189 mm	No. of Blades	6
$D$	375 mm	$(P/D)_{mean}$	0.935
$C_b$	0.662	$A_e/A_o$	1.003
Scale Ratio	36	$K_T$	0.2003

**Table 2:** Test conditions of experiments

Propeller	Position					$V_T$ (m/s)
	$-0.40R^*$	$-0.28R$	$-0.00R$	$+0.28R$	$+0.4R$	
x	X	x	o	x	x	2.1
x	O	o	o	o	o	6.5
o	O	o	o	o	o	6.5

## 2 Experimental investigations

### 2.1 Experimental setup

Wake measurements in large cavitation tunnel of SCAT (Samsung CAvitation Tunnel) are carried out for large size container model as shown in Figure 1. The width and the depth of the test section is 3 m and 1.4 m respectively and the maximum speed of the flow is 15 m/sec. Principal characteristics of the container model and the propeller are shown in Table 1.

Axial velocities are measured using LDV (Laser Doppler Velocimetry) at five planes,  $-0.4R$ ,  $-0.28R$ ,  $0.28R$ ,  $0.4R$  apart from the propeller plane as well as propeller plane. Here,  $R$  denotes the radius of the propeller and the positive sign refers to the downstream from the propeller. LDV probe was set under the bottom of test section and laser beam from the probe projected through bottom window. Since the probe uses 1,139 mm focal length lens, the beam could reach to 20 mm higher than propeller top. Velocities of each plane are measured at 245 points, i.e., 7 radial and

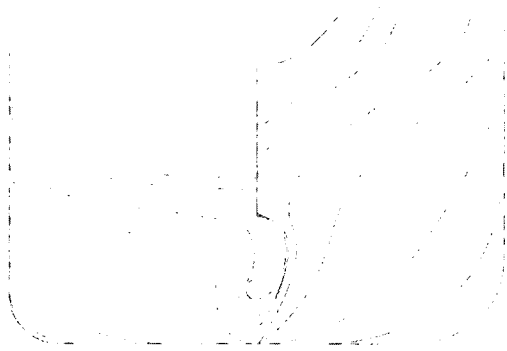


**Figure 1:** Body plan of container model

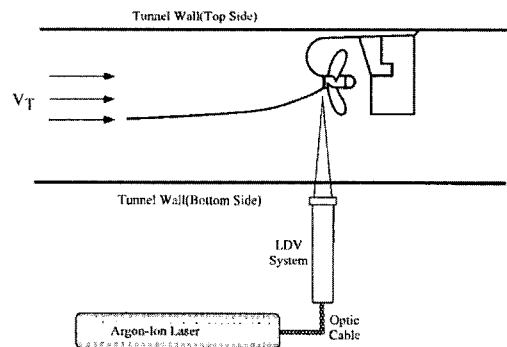


**Figure 2:** Measurement system in SCAT

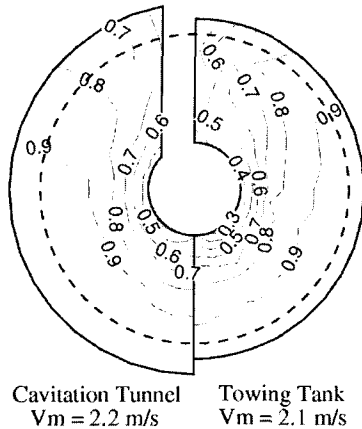


**Figure 3:** Nominal velocities of the model

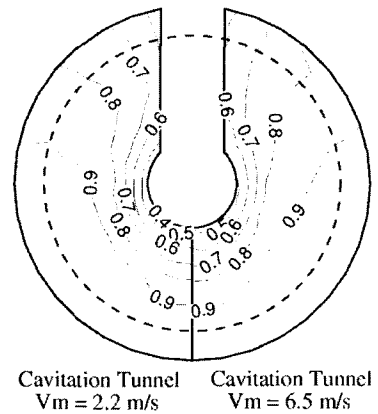


**Figure 4:** Effect of Reynolds number on nominal velocities

35 angular positions for the model with and without propeller. The velocities were decided from the 500 particles (seed) speed average, which detected at each point. So the velocity averaged all speeds varying propeller phase angle.

The conditions of the experiments are summarized in Table 2. Schematic diagram of the experimental setup is shown in Figure 2. All tests are carried out in non-cavitating conditions and the inflow velocity of 2.1 *m/sec*, which is the same of the towing carriage, was selected to compare the results of the towing tank test. Inflow velocity of 6.5 *m/sec*, which is used to visualize the cavity of the propeller was also selected to compare the results of the towing tank.

## 2.2 Experimental results and discussion

To verify the wall effect of the tunnel, nominal velocities are measured in cavitation tunnel and compared to the towing tank results of the model. Both results show similar trends although the flow in the tunnel is accelerated by the wall effect as shown in Figure 3. Figure 4 shows the wake fields to study the effect of Reynolds number on the nominal velocities in the cavitation tunnel. From this figure, the Reynolds number effect is considered not so large as in Huang and Groves (1980) where wake fields in the small tunnel showed similar results obtained in other large cavitation tunnels.

Figure 5 depicts the wake fields of model to clarify the effect of the propeller operation. Time-averaged mean velocities are non-dimensionalized by reference tunnel velocity and dashed line represents the diameter of the propeller. When the propeller is not present, the port and starboard symmetry is shown and the velocities in the lower part of the model increase slowly. However, when the propeller is present, the velocities at the upstream region of the propeller are accelerated by the propeller action. Downstream velocities are also accelerated by the propeller actions for about 30~40 percent and the port and starboard asymmetry is clearly shown within propeller disc region. Furthermore, circumferential velocities are smoothed in the slipstream and relatively small decelerations outside of propeller disc region are obtained as expected.

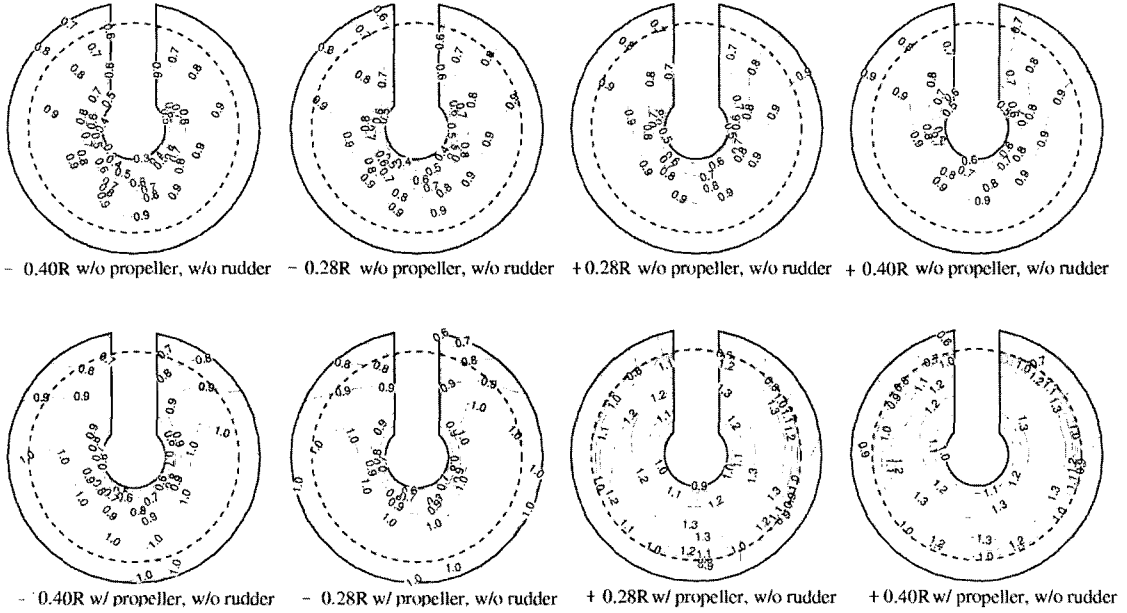


**Figure 5:** Effects of propeller operation on the wake fields

### 3 Numerical simulations

#### 3.1 Simplified vortex ring theory

According to ITTC Propulsor Committee (1984), effective velocity  $u_e$ , calculated from the interaction among the hull, propeller and the rudder, is defined as follows:

$$\underline{u}_e(x) \equiv \underline{u}_t(x) - \underline{u}_i(x) \quad (1)$$

where  $u_e$ ,  $u_t$  and  $u_i$  denote the effective velocity, the total velocity, and the induced velocity by the propeller, respectively. With the assumption of an inviscid and incompressible flow, the effective velocity can be expressed by the following volume integral (Lee et al 1990).

$$\underline{u}_e(x) = \iiint \underline{w}_Q \times \nabla_p(-1/4r\pi)dV + \underline{U} \quad (2)$$

To solve the (2), the vorticity,  $w_Q$  has to be known beforehand. But it varies according to propeller action, so it can be initialized by nominal wake distributions and requires iterative computational procedure to obtain converged effective velocity distributions. Following Lee et al (1990), Kong et al (1998) have computed the effective velocity distributions using slipstream contraction model and the iteration procedures with the streamline tracing method. The former compared their results with measurements of axi-symmetric body while the latter compared with towing tank results based on thrust identity. Computations are made under the assumption of steady and circumferential mean velocity basis and detailed numerical procedure and computation results are described in Kong et al (1998).

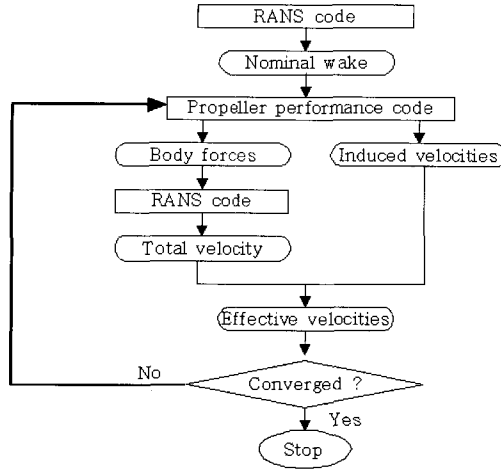


**Figure 6:** Flow chart for RANS solver

### 3.2 RANS solver with body force

Effective velocities are also obtained using the RANS (Reynolds Averaged Navier-Stokes) solver with body forces. In this approach, the propeller is replaced with an actuator disk and its effects are reflected as body forces (axial and tangential direction) following the method of Stern et al (1994).

Since the effective velocity term is directly related to body force distribution of an actuator disk, nominal velocity distribution should be simulated by RANS equation to provide an input for the computations of propeller performance at the first stage. As an initial input data, the vortex ring theory uses the given nominal velocities obtained by the experiments while RANS solver uses computed values without body forces. In order to obtain converged solution, iterative procedure is required and the flow chart of the computations are shown in Figure 6. During the computations, propeller induced velocities and body force distributions are simulated by the unsteady propeller performance code using unsteady vortex lattice method.

The viscous flow method solves the incompressible three-dimensional continuity and RANS equations in conjunction with the pressure Poisson equation and the modified Baldwin-Lomax turbulence model for mean velocity components. The governing equations were expressed as follows:

$$\frac{\partial u_k}{\partial x_k} = 0 \quad (3)$$

$$\frac{\partial u_i}{\partial t} + u_j \frac{\partial u_i}{\partial x_j} = -\frac{\partial}{\partial x_i} \hat{P} + \frac{1}{R_{eff}} \nabla^2 u_i + \frac{\partial \nu_t}{\partial x_j} \left( \frac{\partial u_j}{\partial x_i} + \frac{\partial u_i}{\partial x_j} \right) + F b_i \quad (4)$$

where

$$R_{eff} = \frac{1}{\frac{1}{Re} + \nu_t} \quad (5)$$

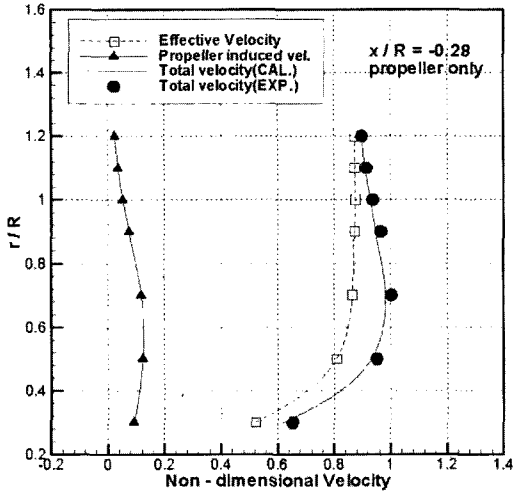


Figure 7: Comparisons of total velocity using VLM ( $x/R = -0.28$ )

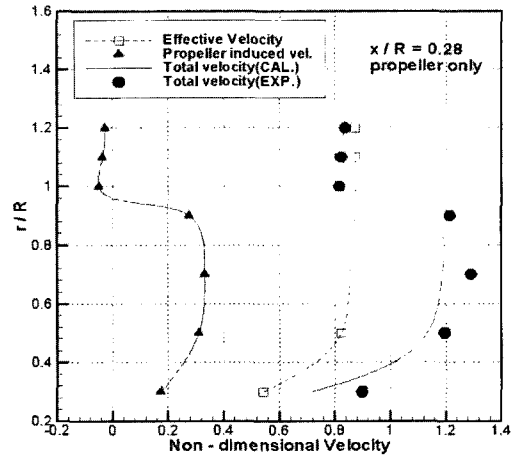


Figure 8: Comparisons of total velocity using VLM ( $x/R = 0.28$ )

and  $F_b$ ,  $Re$  and  $\nu_t$  denote the body force, Reynolds number and the eddy viscosity, respectively.

The present method employed the O-H type non-staggered grid system and uses the second order finite differences for the space and the four-stage Runge-Kutta time stepping scheme for the temporal discretizations. The numerical analysis of propeller-hull interaction is carried out for practical container ship. The corresponding Reynolds number is  $1.0e7$ , which is similar to that of towing tank test. The computational domains are extended one ship length  $L$  downstream and  $0.6L$  in both depth and width, and the mid ship is selected as an inlet section of the computational domain.

### 3.3 Numerical results and discussion

Total velocities computed with the above two methods are compared with the experiments at two measuring planes. Total velocities at the propeller upstream and downstream are shown in Figures

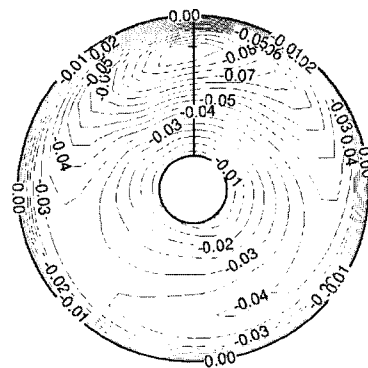
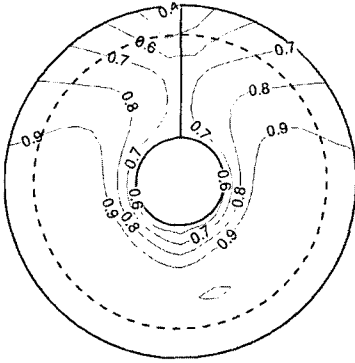
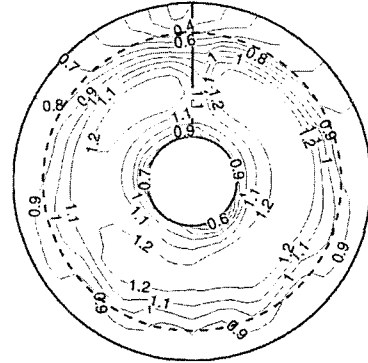


Figure 9: Body force distributions at  $+0.0R$



**Figure 10:** Total velocity contours by RANS solver ( $x/R = -0.28$ , propeller operating)



**Figure 11:** Total velocity contours by RANS solver ( $x/R = 0.28$ , propeller operating conditions)

7 and 8. Although the simplified vortex ring theory is applied, the computed results show good agreements with the measured ones even in propeller working conditions. Figure 9 shows the axial body force distributions obtained by the propeller performance code using the computed nominal wake. In RANS solver, effective velocities converged with four iterations. Total velocity contours obtained by the RANS computation are shown in Figures 10 and 11 at different planes. Although the RANS solver still can't simulate the model test results quantitatively, computed results seem to be reasonable compared to the measured data shown in Figure 5. In Figures 12 and 13, circumferential mean axial velocities by the RANS solver and VLM method are compared with the experimental data. RANS solver results show poorer agreement than the simplified vortex ring method, however, the general trends follow the experimental results. The RANS solver may

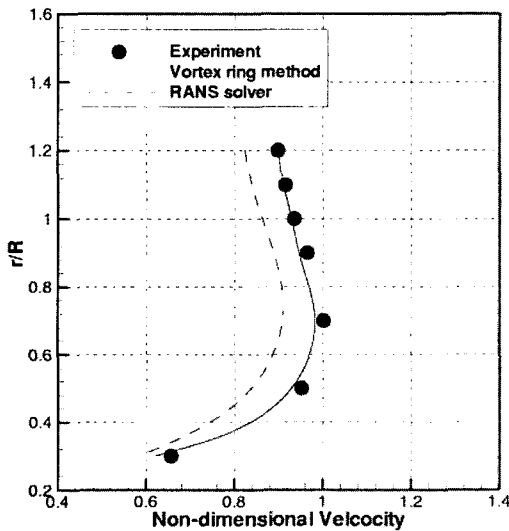


**Figure 12:** Total velocity comparison ( $x/R = -0.28$ )

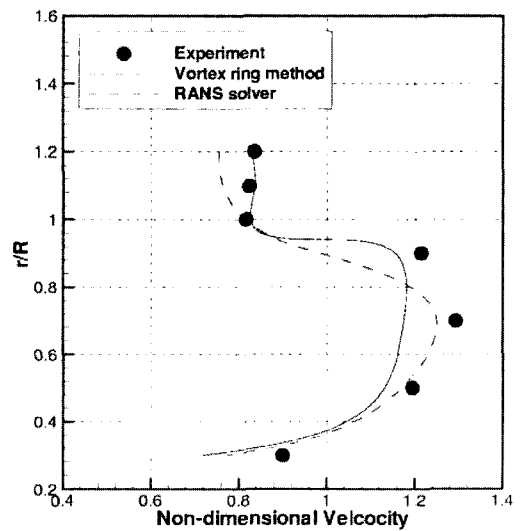


**Figure 13:** Total velocity comparison ( $x/R = 0.28$ )

therefore be a useful substitute as a design tool at the initial stage, because the effective velocities are obtained by the pure computations whereas the simplified vortex ring method requires nominal velocities which can be obtained from the expensive and time-consuming model tests.

## **4 Concluding remarks**

LDV measurements around a propeller in action are carried out to provide valuable information for more accurate wake-adapted propeller design and to study hull-propeller interactions. Although simplified vortex ring theory has critical limitations, i.e., nominal velocities should be known beforehand by the experiment or computational method, the computed effective velocities using the measured nominal velocities show good agreements with experimental data. As an alternative design tools at preliminary design stage, RANS solver with body force showed qualitative agreement with experiments. The RANS solver should be developed to obtain more accurate solutions and to have the capability of high Reynolds number computations. Since the time averaged mean velocities are measured only in the LDV measurements, all data could not show phase or velocity fluctuations caused by the rotation of propeller blades. Tangential and radial velocities and phase measurement should be studied in the near future. It would also be important to consider the unsteadiness of the hull and propeller interactions in computations.

## **Acknowledgements**

This work is a part of a project supported by the Korean Science and Engineering Foundation, Contract R11-2002-008-04003-0.

## **References**

- BRESLIN, J.P., KERWIN, J. AND JOHNSON, C.A. 1980 Theoretical and Experimental Propeller Induced Hull Pressure Arising from Intermittent Blade Cavitation, Loading and Thickness. *T. of SNAME*, **90**, pp. 111-151
- CORDIER, S., BRIANCON-MARJOLLET, L., LAURENS, J.M. AND RAULO, J. 1995 Effect of wake scaling on the prediction of propeller cavitation. DCN Bassin d'Essais des Carenes VAL DE REUIL, International Symposium on Cavitation, CAV95
- HUANG, T.T. AND GROVES, N.C. 1980 Effective wake: Theory and Experiment. 13th Symposium on Naval Hydrodynamics, Tokyo, pp. 651-673
- KONG, D.S., KIM, Y.G. AND LEW, J.M. 1998 On the practical computation of propulsion factors of ships. *Practical Design of Ships and Mobile Units*
- LEE, C.S., KIM, Y.G. AND AHN, J.W. 1990 Interaction between a propeller and the stern shear flow. *Proc of Korea-Japan Joint Workshop On Hydrodynamics in Ship Design*, Seoul, Korea
- Report of Propeller Committee. 1984 *Proc of 17th International Towing tank conference*
- STERN, F., KIM, H.T., ZHANG, D.H., TODA, Y., KERWIN, J. AND JESSUP, S. 1994 Computation of viscous flow around propeller body configurations: Series 60 CB = 0.6 Ship model. *J. of ship research*, **38**, **2**, pp. 137-157